

p53 and ATM/ATR Regulate 7,12-Dimethylbenz[a]anthracene-Induced Immunosuppression

Jun Gao, Leah A. Mitchell, Fredine T. Lauer, and Scott W. Burchiel

The University of New Mexico College of Pharmacy Toxicology Program, Albuquerque, New Mexico

Received June 22, 2007; accepted October 9, 2007

ABSTRACT

The tumor suppressor protein p53 is a transcription factor that regulates apoptotic responses produced by genotoxic agents. Previous studies have reported that 7,12-dimethylbenz[a]anthracene (DMBA)-induced bone marrow toxicity is p53-dependent *in vivo*. Our laboratory has shown that DMBA-induced splenic immunosuppression is CYP1B1- and microsomal epoxide hydrolase (mEH)-dependent, demonstrating that the DMBA-3,4-dihydrodiol-1,2-epoxide metabolite (DMBA-DE) is probably responsible for DMBA-induced immunosuppression. DMBA-DE is known to bind to DNA leading to strand breaks. Therefore, we postulated that a p53 pathway is required for DMBA-induced immunosuppression. In the present studies, our data show that activated p53 accumulated in the nuclei of spleen cells in WT and AhR-null mice after DMBA treatment, but not in CYP1B1-null or mEH-null mice. These results suggest that DMBA activates p53 in a CYP1B1- and mEH-dependent manner *in vivo*

but is not AhR-dependent. Ataxia telangiectasia mutated (ATM) and ATM and Rad3-related protein (ATR) are sensors for DNA damage that signal p53 activation. Increased ATM, phospho-ATM (Ser¹⁹⁸⁷), and ATR levels were observed after DMBA treatment in WT, p53-null, and AhR-null mice but not in CYP1B1-null or mEH-null mice. Therefore, ATM and ATR seem to act upstream of p53 as sensors of DNA damage. *Ex vivo* immune function studies demonstrated that DMBA-induced splenic immunosuppression is p53-dependent at doses of DMBA that produce immunosuppression in the absence of cytotoxicity. High-dose DMBA cytotoxicity may be associated with p53-independent pathways. This study provides new insights into the requirement of genotoxicity for DMBA-induced immunosuppression *in vivo* and highlights the roles of ATM/ATR in signaling p53.

Polycyclic aromatic hydrocarbons (PAHs) are environmental pollutants that are present as products of incomplete combustion of fossil fuels and other organic matter. Most of the members in the PAH family are potent toxicants and can produce cytotoxic, carcinogenic, and immunotoxic effects (Pelkonen and Nebert, 1982; Uno et al., 2004) in various species, tissues, and cell types (Thurmond et al., 1988; Burchiel et al., 1990; Buters et al., 1999, 2003; Sugiyama et al., 2002). 7,12-Dimethylbenz[a]anthracene (DMBA) has been widely used as a model compound for carcinogenic, immunotoxic, and teratogenic studies (Ikegawonu et al., 1999). Our previous studies have shown that

DMBA suppresses both humoral and cell-mediated immune responses (Burchiel et al., 1990). However, the precise molecular mechanism by which DMBA produces immunosuppression is still not well understood.

Our laboratory has recently demonstrated that deletion of cytochrome P450 1B1 (CYP1B1) (Gao et al., 2005) and microsomal epoxide hydrolase (mEH) (Gao et al., 2007) protects mice against spleen cell immunosuppression produced by DMBA *in vivo*. Thus, CYP1B1 and mEH are associated with the formation of DMBA metabolites responsible for immunosuppression. Based on these observations and other reports (Heidel et al., 2000) and as depicted in Fig. 1, it is clear that DMBA must first be metabolized by CYP1B1 to produce DMBA-3,4-epoxide followed by conversion by mEH to DMBA-3,4-dihydrodiol, and final conversion to the active immunosuppressive metabolite DMBA-3,4-dihydrodiol-1,2-epoxide (DMBA-DE) to produce immunotoxicity. DMBA-DE is believed to be responsible for the immunosuppressive properties of DMBA because it covalently

This work was supported by National Institutes of Health grant R01-ES05495, and the New Mexico Center for Environmental Health Sciences was supported by center grant P30-ES012072 from the National Institute of Environmental Health Sciences.

Article, publication date, and citation information can be found at <http://molpharm.aspetjournals.org>.
doi:10.1124/mol.107.039230.

ABBREVIATIONS: PAH, polycyclic aromatic hydrocarbon; DMBA, 7,12-Dimethylbenz[a]anthracene; mEH, microsomal epoxide hydrolase; DMBA-DE, DMBA-3,4-dihydrodiol-1,2-epoxide; AhR, aryl hydrocarbon receptor; ATM, ataxia telangiectasia mutated; ATR, ATM and Rad3-related; Con A, Concanavalin A; LPS, lipopolysaccharide; WT, wild-type; CO, corn oil; TBS/T, Tris-buffered saline containing Tween 20; HRP, horseradish peroxidase; NK, natural killer cells; FITC, fluorescein isothiocyanate; APC, allophycocyanin; PE, phycoerythrin; PFC, plaque-forming cell; SRBC, sheep red blood cell.

binds to DNA and causes DNA damage (Dipple and Nebzyski, 1978). Therefore, this genotoxic pathway may be the primary mechanism associated with DMBA-induced immunosuppression.

After exposure to genotoxic stimuli, cells will trigger complex signaling pathways in an attempt to maintain genomic stability. A key sensor responsible for DNA damage is p53, a tumor suppressive protein whose loss of function leads to tumor development (Lakin and Jackson, 1999). p53 expression is normally constitutively expressed at low levels in mammalian cells, with a short half-life being regulated by the mouse double minute (mdm) 2 protein (Prives and Hall, 1999). In response to DNA damage, p53 accumulates in the nucleus and becomes activated after phosphorylation. Activated p53 regulates numerous downstream signals such as DNA repair, cell cycle arrest, and apoptosis (Caspari, 2000; Hickman et al., 2002; Roos and Kaina, 2006). Phosphorylation of murine p53 at serine 18 (homologous to human p53 at serine 15) is a key step in the activation of p53 in response to signals of DNA damage (Chao et al., 2000; Appella and Anderson, 2001).

Recent investigations by Page et al. (2003) have shown that DMBA-induced murine bone marrow toxicity is dependent on p53 activation in vivo. In the absence of p53 in null mice, DMBA treatments did not alter bone marrow cell populations or produce hematotoxicity. Based on bone marrow toxicity evidence, we hypothesized that p53 is a critical regulator of DMBA-induced spleen cell immunosuppression. In the present study, we measured p53 levels in splenocyte nuclear protein extracts from wild-type (WT), CYP1B1-null, mEH-null, and aryl hydrocarbon receptor (AhR)-null mice after DMBA treatments. Moreover, we detected the ataxia telangiectasia mutated (ATM), and ATM and Rad3-related (ATR) protein levels in nuclear extracts in splenocytes (Keegan et al., 1996; Gately et al., 1998). ATM and ATR are members of the phosphoinositide 3-kinase family that are known to be critical sensors that initiate cellular genotoxic response after double-strand DNA breaks (Shiloh, 2003; Yang et al., 2003). Studies have shown that ATM can be rapidly activated after genotoxic insult and can phosphorylate and stabilize murine p53 Ser¹⁸ (Banin et al., 1998; Canman et al., 1998). Whereas, ATR activation is a later response that maintains p53 Ser¹⁸ phosphorylation (Tibbetts et al., 1999; Myers and Cortez, 2006). ATM and ATR are key regulators of p53 phosphorylation in vivo (Lavin et al., 2005).

Furthermore, activation of ATM results from phosphorylation of Ser¹⁹⁸⁷ in response to DNA damage (Bakkenist and Kastan, 2003; Kurz and Lees-Miller, 2004). The involvement of ATM and ATR in DMBA-induced immunotoxicity has not been previously reported.

The present study demonstrates that ATM and ATR are phosphorylated after exposure of WT mice to DMBA, but not in CYP1B1 or mEH-null mice. These results suggest that DMBA-DE is important in the activation of ATM/ATR. In addition, we show that p53-null mice are protected from DMBA-induced immunotoxicity, demonstrating that genotoxicity is a major mechanism of immunotoxicity.

Materials and Methods

Chemicals and Reagents. All solvents and reagents used were of analytical or HPLC grade. 7,12-Dimethylbenz[a]anthracene (greater than 95% purity), Concanavalin A (Con A; Type IV), and corn oil were purchased from Sigma-Aldrich (St. Louis, MO). Lipopolysaccharide (LPS) from *Escherichia coli* was purchased from Alexis Biochemicals (San Diego, CA). Cell culture reagents were from Sigma-Aldrich and Invitrogen (Grand Island, NY).

Animals. In this report, WT C57BL/6N, CYP1B1-null, mEH-null, AhR-null, and p53-null mice (*Trp53^{tm1Tyx}*) were used to investigate the role of p53 in DMBA-induced immunotoxicity. Female wild-type C57BL/6N mice (6–8 weeks old) were purchased from Harlan Laboratories (Indianapolis, IN) and male wild-type C57BL/6J mice (6–7 weeks old) were obtained from The Jackson Laboratory (Bar Harbor, ME). CYP1B1-null, mEH-null, and AhR-null mice breeders with C57BL/6N genetic background were received from the National Institutes of Health (Bethesda, MD). The p53-null mice breeders were purchased from The Jackson Laboratory. These knockout mice were bred in our Association for Assessment and Accreditation of Laboratory Animal Care (AAALAC)-accredited animal facility under an Institutional Animal Care and Use Committee-approved protocol. All knockout mice were confirmed using a polymerase chain reaction genotyping method with DNA isolated from tail snips (Jacks et al., 1994; Miyata et al., 1999). The male p53-null mice used for the immune function studies were 10 to 14 weeks old, and the male wild-type (C57BL/6J) mice were 11 to 12 weeks old when used as controls. p53-null mice were checked daily to monitor for visible tumor development. No animals bearing tumors were used in these studies. In all of the experiments, mice were orally gavaged with corn oil (CO; vehicle control) or DMBA once a day for 5 days, using five mice per group. The cumulative doses of DMBA were 17, 50, and 150 mg/kg. Forty-eight hours after the last DMBA treatment, animals were euthanized by CO₂ narcosis. Spleens were aseptically isolated and divided into two parts. One half of the spleen was held on ice in

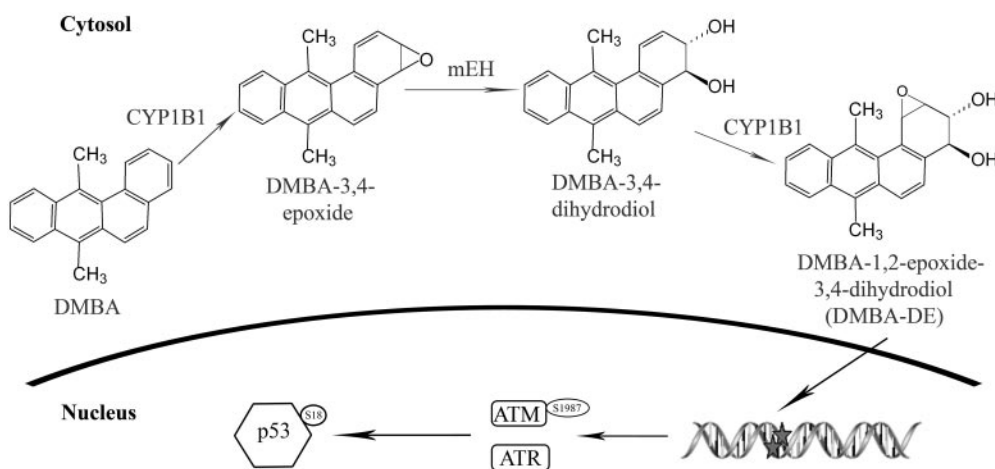


Fig. 1. Schematic for DMBA metabolism and the formation of the ultimate genotoxic metabolite of DMBA, DMBA-DE.

sterile Hanks' balanced salt solution for immune function assays. The preparation of spleen cell suspension has been described previously (Gao et al., 2005). The remaining half of spleen was immediately frozen in liquid nitrogen and then stored at -80°C for Western blot analyses.

Preparation of Nuclear Protein Extraction. To prepare the nuclear protein extraction, spleen snips were homogenized in 200 μl of lysis buffer A supplemented with protease inhibitors (containing 10 mM HEPES, 1.5 mM MgCl_2 , 10 mM KCl, 0.5 mM dithiothreitol, 0.03% Nonidet P-40, 0.4 mM phenylmethylsulfonyl fluoride, 1 units/ml aprotinin, and 10 $\mu\text{g}/\text{ml}$ leupeptin, pH 7.9). Samples were held on ice for 10 min and then centrifuged at 4°C , 6000 rpm for 5 min. The supernatant was discarded, and pellets were washed one time with 200 μl of lysis buffer A. Samples were again centrifuged at 4°C , 6000 rpm for 5 min and the pellets, containing nuclei, were collected to prepare the nuclear protein extract. The pellets were resuspended in 50 μl of lysis buffer B (containing 20 mM HEPES, 0.45 M NaCl, 1.5 mM MgCl_2 , 0.2 mM EDTA, 0.1 mM EGTA, 25% glycerol, 0.5 mM dithiothreitol, 0.4 mM phenylmethylsulfonyl fluoride, 1 units/ml aprotinin, 10 $\mu\text{g}/\text{ml}$ leupeptin, and 3 $\mu\text{g}/\text{ml}$ pepstatin A, pH 7.9). Suspensions were mixed on a LabQuake shaker for 15 min at 4°C and centrifuged at 14,000 rpm for 5 min at 4°C . The supernatants, containing nuclear proteins, were held in 0.65-ml microcentrifuge tubes. The nuclei pellets were washed with 30 μl of lysis buffer B then centrifuged at 14,000 rpm for 5 min at 4°C . The supernatants were again collected and combined with the first collection and stored at -80°C . Total protein concentrations were determined using Protein Assay reagent (Bio-Rad Laboratories, Hercules, CA).

Western Blot Analysis. To analyze the total p53, phospho-p53 (Ser¹⁸), ATM, and ATR expression, 200 μg of nuclear protein extract was heated to 95 – 100°C for 5 min with equal volumes of Laemmli sample buffer (Bio-Rad Laboratories). For total p53 and phospho-p53 (Ser¹⁸) analysis, samples were separated by SDS polyacrylamide gel electrophoresis using a 10% gel with a 5% stacking gel using a mini-PROTEAN 3 cell system (Bio-Rad Laboratories). After 1-h electrophoresis at 180 V, the proteins were transferred for 1 h using a constant 300-mA current to nitrocellulose membranes (0.45 μm ; Bio-Rad Laboratories). Nonspecific binding was blocked by incubating membranes in 5% (w/v) nonfat dry milk in Tris-buffered saline containing Tween 20 [TBS/T; 50 mM Tris, pH 7.4, 150 mM NaCl, and 0.1% (v/v) Tween 20] at room temperature for 1 h. Incubation was followed by three 5-min TBS/T washes; membranes were then incubated with a polyclonal phospho-p53 (Ser¹⁸) antibody (1:1000; Cell Signaling Technology Inc., Danvers, MA) at 4°C overnight. After washing with TBS/T, membranes were incubated with a horseradish peroxidase (HRP)-conjugated anti-rabbit IgG secondary antibody (1:1000; Cell Signaling Technology Inc.) for 1 h at room temperature. The protein bands were detected using a Western Lightning Chemiluminescence Reagent (PerkinElmer Life and Analytical Sciences, Waltham, MA) and resolved on a Kodak Image Station 4000 mm (Eastman Kodak, Rochester, NY). The protein molecular weight was determined by comparison with Precision Plus Protein Prestained Standards (Bio-Rad Laboratories). After detection of bands by imaging, the blots were stripped of antibodies using a buffer [containing 7 M guanidine HCl, 0.1 M KCl, 0.05 M glycine, 0.05 mM EDTA, and 0.14% (v/v) 2-mercaptoethanol, pH 10] and were reprobed with a p53 1C12 antibody (1:2000; Cell Signaling Technology) or histone-H1 (1:500; Santa Cruz Biotechnology, Santa Cruz, CA).

For ATM and ATR detection, nuclear protein extractions (200 μg) were resolved on 5% SDS-polyacrylamide gels with 4% stacking gel and then transferred to polyvinylidene difluoride membranes (0.45 μm ; PerkinElmer Life and Analytical Sciences) for 2.5 h with a constant current of 400 mA. The membranes were incubated with ATM (2C1 clone, 1:500; Santa Cruz Biotechnology), phospho-ATM (Ser¹⁹⁸⁷) (10H11.E12 clone, 1:1000; Cell Signaling Technology), ATR (1:500; Santa Cruz Biotechnology), or a loading control β -tubulin (clone, 1:500; Santa Cruz Biotechnology), at 4°C overnight. After

washing with TBS/T, the membranes were incubated with the appropriate secondary antibodies: goat anti-mouse IgG-HRP (1:2000) or goat anti-rabbit IgG-HRP (1:2000). The detection of protein bands is described above. The molecular weights of the protein bands were determined using HiMark prestained high molecular weight protein standards (Invitrogen, Carlsbad, CA).

Flow Cytometric Analyses. Spleen cells were prepared as described previously (Gao et al., 2005). To characterize the subtype of lymphocytes, spleen cells were stained by specific cell surface markers [pan-T (CD3), Th (CD4), Tc (CD8) cells, B cells (CD19), natural killer (NK) cells (CD16), macrophages (Mac-1)]. Three custom rat anti-mouse monoclonal antibody cocktails were purchased from BD Pharmingen (San Diego, CA), including IgG1+IgG2a-FITC/IgM-PE/CD45-PerCP/IgG2a-APC, CD3-FITC/CD8a-PE/CD45-PerCP/CD4-APC, and CD3+CD19-FITC/Pan NK-PE/CD45-PerCP/Mac-1APC. The cell-staining procedure has been described previously (Gao et al., 2005). In brief, mouse spleen cells (1×10^6 cells/mouse) were aliquoted into three 12×75 -mm flow tubes and incubated with purified rat anti-mouse CD16/CD32 monoclonal antibody (Fc block antibody; BD Pharmingen) for 10 min at room temperature in the dark. Twenty microliters of antibody cocktail was then added to the appropriate sample tube and incubated for 30 min in the dark. Fresh $1 \times$ ammonium chloride (2 ml/sample) was added for 10 min at room temperature in the dark to lyse red blood cells. After centrifugation at 275g for 10 min, supernatants were discarded. Cell pellets were washed with 2 ml of the phosphate-buffered saline wash buffer (Sigma Chemical Co, St. Louis, MO) (containing 0.09% sodium azide and 1% fetal bovine serum) and then centrifuged. Finally, cells were resuspended in 400 μl of phosphate-buffered saline wash buffer. Samples were analyzed on a FACSCalibur Flow Cytometry system (BD Biosciences).

To characterize the role of p53 in vivo, the spleen cells from corn oil control or DMBA-treated male wild-type (WT) C57BL/6J and p53-null mice were used for immune function assays. In this report, three major immune function assays were performed as listed below.

T-Dependent Antibody Response Measured by the Plaque-Forming Cell Assay. The primary IgM response to T-dependent antigen, sheep red blood cells (SRBC) was assessed as described previously (Gao et al., 2005). In brief, mouse spleen cells (2×10^6 cells/ml, 0.5 ml) were immunized with equal volume of 1% SRBC (Colorado Serum, Denver, CO) ex vivo for 4 days using a modified Mishell-Dutton culture system. The number of PFC were counted after a 4-day incubation in a humidified, 5% CO_2 , 37°C incubator using a glass slide modification of Jerne and Nordin PFC assay (Gao et al., 2005). In brief, immunized spleen cells or control cells were mixed with 50 μl of a 50% SRBC suspension and 400 μl of 43°C prewarmed 0.8% Seaplaque agarose (Intermountain Scientific, Kaysville, UT), and was poured onto 0.15% Seaplaque agarose pre-coated microscope slides. After 1-h incubation in a humidified 37°C (without CO_2) incubator, slides were flooded with diluted guinea pig complement [1:20 (v/v); Dulbecco's phosphate-buffered saline containing calcium and magnesium; Colorado Serum, Denver, CO]. Slides were then incubated for 2 h at 37°C , and the number of anti-SRBC PFCs was identified using a Bausch and Lomb dissecting microscope. Results are expressed as the number of PFCs per total number of cultured cells.

[^3H]Thymidine Incorporation Mitogenesis Assay. Cell mitogenesis assays were performed using two mitogens, lipopolysaccharide (LPS) for B cell proliferation and Con A for T-cell proliferation. Mouse spleen cells (1×10^6 cells/ml, 200 μl) were cultured in complete RPMI 1640 medium (supplemented with 10% fetal bovine serum, 2 mM L-glutamine, 100 $\mu\text{g}/\text{ml}$ streptomycin, and 100 units/ml penicillin) with LPS at 10 $\mu\text{g}/\text{ml}$ or Con A at 1 $\mu\text{g}/\text{ml}$ or medium for 2 days in 96-well culture plates. Spleen cells plated in complete RPMI 1640 medium without mitogens served as controls to monitor spontaneous proliferation. Replicates of six cultures were used for each mitogen and each mouse spleen sample. After 48 h of incubation at 37°C in a humidified, 5% CO_2 incubator, 20 μl of 50 $\mu\text{Ci}/\text{ml}$

[³H]thymidine (MP Biomedical, Irvine, CA) was added to each well, and plates were then incubated for 18 h in a humidified, 37°C, 5% CO₂ incubator. Samples were then harvested onto glass filters using a Brandel model 24V cell harvester, and filters were transferred to liquid scintillation vials containing 3 ml of ScintiVerse BD cocktail (Thermo Fisher Scientific, Waltham, MA). The incorporated [³H]thymidine for each sample was determined by liquid scintillation counting (Beckman Coulter, Fullerton, CA). Proliferation in response to LPS and ConA are expressed as counts per minute.

Natural Killer Cell ⁵¹Cr Assay. The NK activity was determined by measuring chromium (⁵¹Cr) release from the NK-sensitive Yac-1 target cells (American Type Culture Collection, Manassas, VA). Yac-1 target cells (T) (2 × 10⁶ cells) were labeled with 1.0 mCi Na₂⁵¹CrO₄ (⁵¹Cr) (PerkinElmer Life and Analytical Sciences) for 1 h in a humidified, 37°C, 5% CO₂ incubator. The labeled cells were then washed twice with 10 ml of DPBS and adjusted to the concentration of 5 × 10⁴ cells/ml and held in a humidified, 37°C, 5% CO₂ incubator. Spleen cells (100 μl) were plated as effector (E) cells in round-bottomed, 96-well culture plates (Corning Inc., Corning, NY) in triplicate. ⁵¹Cr-labeled target cells (100 μl) were added to each well. The effector-cell-to-target-cell ratios were 200:1, 100:1, 50:1, and 25:1. The first 12 wells on each culture plate contained target cells alone in complete RPMI 1640 medium (six wells) and target cells in medium containing 5% Triton X-100 (six wells). These controls served for spontaneous and maximal ⁵¹Cr release, respectively. After 4-h incubation in a humidified, 37°C, 5% CO₂ incubator, plates were centrifuged at 275g for 5 min at 4°C. One hundred microliters of the supernatant was harvested from each well, and the radioactivity was detected with a Wallac 1480 WIZARD gamma counter. The data were expressed as percentage of lysis: % lysis = [(mean sample ⁵¹Cr release cpm – mean spontaneous ⁵¹Cr release cpm)/(mean maximum ⁵¹Cr release cpm – mean spontaneous ⁵¹Cr release cpm)] × 100.

Statistical Analyses. Data were analyzed by SigmaStat software (Systat Software, Inc., San Jose, CA). The statistical differences among groups were determined by one-way analysis of variance and/or Student's *t* test. The values were expressed as mean ± S.E.M. A *p* value < .05 indicated a statistically significant difference.

Results

DMBA Caused p53 Accumulation in the Nucleus of Spleen Cells from WT Mice. To evaluate the cellular p53 response to DMBA-induced genotoxic stress in splenocytes, cytoplasmic and nuclear protein extracts isolated from spleen cells were prepared from corn oil- and DMBA-treated female WT mice. Western blot analyses demonstrated a DMBA dose-dependent (17–150 mg/kg) increase in the amount of p53 protein accumulated in the nucleus of spleen cells (Fig. 2A, left). However, the cytoplasmic p53 protein levels were almost nondetectable after DMBA treatment (Fig. 2A, right), indicating that DMBA did not alter the p53 translational level. Increased nuclear p53 levels may be produced by post-translational modification (Appella and Anderson, 2001) or mdm2 modification (Meek and Knippschild, 2003), which can result in decreased p53 degradation. Phospho-p53 (Ser¹⁸) was detected in nuclear protein extractions as well (Fig. 2A, left). The induction of phospho-p53 (Ser¹⁸) was increased 2.2- to 4.7-fold by DMBA treatment compared with the corn oil control. Phosphorylated p53 was not detected in the cytoplasmic fraction (Fig. 2A, right). These results demonstrate that DMBA treatments cause p53 accumulation in the nucleus and can lead to activation of p53 by phosphorylation at serine 18. Similar Western blot results were obtained in male mice after DMBA treatment (Fig. 6A).

ATM and ATR are well known to act as upstream regula-

tors of p53 and sensors of DNA damage (Yang et al., 2003; Kurz and Lees-Miller, 2004). In this report, we measured ATM, phospho-ATM (Ser¹⁹⁸⁷), and ATR protein levels in the nucleus after DMBA treatments compared with corn oil-exposed control mice (Fig. 2B). The ATM levels increased ~1.9-fold in WT female mice at the 50 mg/kg DMBA dose and ~3.6 fold in WT male mice. Furthermore, phospho-ATM (Ser¹⁹⁸⁷) and ATR levels were up-regulated by DMBA treatments in both WT female and male mice. These results demonstrate that DMBA increases ATM and ATR protein levels in the nucleus, and enhance the phosphorylation of ATM at serine 1987.

p53 Activation Was CYP1B1-Dependent In Vivo. In a previous study, we examined the immunosuppressive effects of DMBA in CYP1B1-null mice (Gao et al., 2005). DMBA does not produce immunosuppression in CYP1B1 knockout mice exposed in vivo, and therefore CYP1B1 is a critical enzyme for metabolic activation of DMBA (Fig. 1). We therefore determined whether DMBA produced changes in p53 nuclear protein levels in the spleen cells from DMBA-treated CYP1B1-null mice (Fig. 3A). WT mice treated with corn oil or 150 mg/kg DMBA were used as the control groups. As expected, total p53 protein levels in the nucleus did not increase after DMBA treatments compared with the WT mice or the corn oil-treated CYP1B1-null mice. The phospho-p53 (Ser¹⁸) signal was observed only in the WT mice treated with 150 mg/kg DMBA and was not detected in CYP1B1-null mice. These data demonstrate that the p53 activation in-

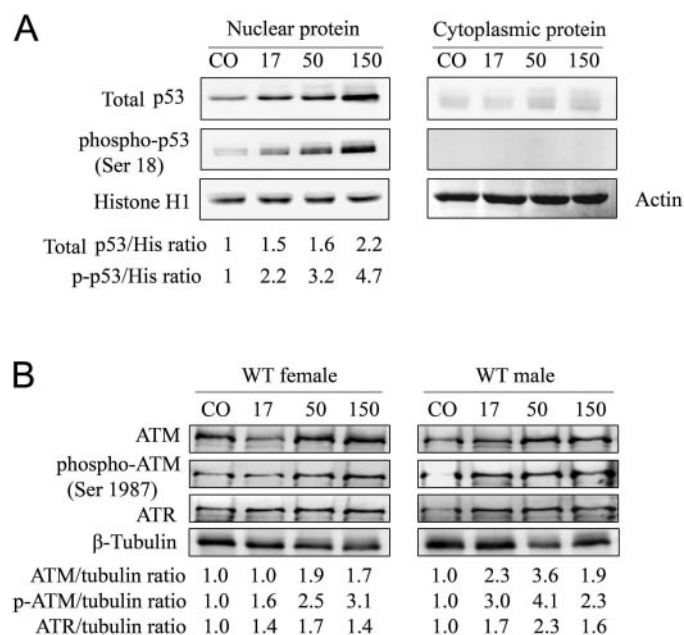


Fig. 2. p53, ATM, and ATR are activated by DMBA treatments in WT mice. A, total p53 and phospho-p53 (Ser¹⁸) levels in nuclear fraction and cytoplasmic fraction were analyzed by Western blot. Histone H1 and actin were used as protein loading controls for nuclear protein and cytoplasmic protein extraction, respectively. The normalized total p53 and phospho-p53 (Ser¹⁸) levels measured by densitometry analysis are indicated as total p53/His ratio:total p53/histone ratio. Phospho-p53/his ratio:phospho-p53/histone H1 ratio. B, ATM, phospho-ATM (Ser¹⁹⁸⁷), and ATR levels were measured in nuclear protein extractions of WT female and male mice after DMBA and CO treatments. The normalized density of lanes is indicated as a ratio at the bottom of each blot. The densitometry analysis used β-tubulin protein as a loading control. 17, 50, and 150 indicate 17, 50, and 150 mg/kg DMBA, respectively.

duced by DMBA is CYP1B1-dependent and that if DMBA cannot be metabolized by CYP1B1, it cannot trigger the downstream target p53.

We next measured the overall levels of ATM and ATR levels in CYP1B1-null mice treated with corn oil or 17 to 150 mg/kg DMBA (Fig. 3B). The levels of ATM, phospho-ATM (Ser¹⁹⁸⁷) and ATR remained at baseline after the DMBA treatments compared with the corn oil control. Thus, these results demonstrate that total levels of ATM and ATR are not changed after treatment of CYP1B1-null mice with DMBA.

Loss of Functional mEH Protein Prevented p53 Up-Regulation in Response to DMBA Treatments. To further elucidate the signaling pathway responsible for p53 activation in vivo, mEH-null mice were used to determine the levels of p53 protein after DMBA treatments. We previously observed that mEH-null mice are resistant to the DMBA-induced immunosuppression, similar to CYP1B1 mice (Gao et al., 2007). The levels of total p53 in the nucleus from DMBA-treated mEH-null mice were determined by Western blot analysis, and a control group of WT mice were also included (Fig. 4A). The normalized densitometric results with corresponding levels of histone H1 show that whereas DMBA increased p53 nuclear protein levels in WT mice, there was no p53 response in mEH-null mice. After DMBA treatment of WT mice, a strong phosphorylation signal for p53 serine 18 was observed. Again, this response was absent in the mEH-null mice (Fig. 4A). In mEH-null mice, there was also no detectable change in the total levels of ATM and ATR or the phosphorylation of ATM serine 1987 (Fig. 4B). The normalized band intensities of ATM, phospho-ATM (Ser¹⁹⁸⁷), and ATR remained unchanged after DMBA treatment in mEH-null mice. These results indicate that mEH is another

key enzyme required for the metabolism of DMBA and activation of ATM, ATR, and p53.

Lack of Influence of the AhR on DMBA Activation of p53, ATM, and ATR. The AhR has been shown to be involved in the pathways of metabolic activation for many PAHs, such as benzo[a]pyrene (Dertinger et al., 2001). However, immune function studies conducted in our laboratory have shown that DMBA can produce immunosuppressive effects in AhR-null mice (data not shown). Thus, AhR is not necessary for DMBA-induced immunosuppression. To further investigate this phenomenon, we analyzed spleen cell nuclear p53, ATM, and ATR activity by Western blot in AhR-null mice after DMBA treatments. As shown in Fig. 5A, the increase in p53 protein levels produced by DMBA treatment was observed in the WT group as well as in the AhR knockout mice. WT mice given corn oil and 150 mg/kg DMBA treatments were used as negative and positive controls, respectively. In AhR-null mice, we observed that the nuclear ATM protein level was up-regulated from 2.2- to 4.4-fold by DMBA treatment (Fig. 5B). The phospho-ATM (Ser¹⁹⁸⁷) level increased from 1.6- to 2.7-fold after DMBA treatment. The nuclear ATR protein level was enhanced ~3.0-fold by DMBA treatment. The induction of these proteins by DMBA was found to be dose-dependent. These results suggest that the absence or presence of AhR does not influence the activation of p53, ATM, and/or ATR in spleen cells.

DMBA Activation of ATM and ATR in p53-Null Mice. To further evaluate the effect of DMBA on activation of p53, ATM and ATR, we investigated the p53, ATM, and ATR protein levels in p53-null mice. As shown in Fig. 6A, total p53

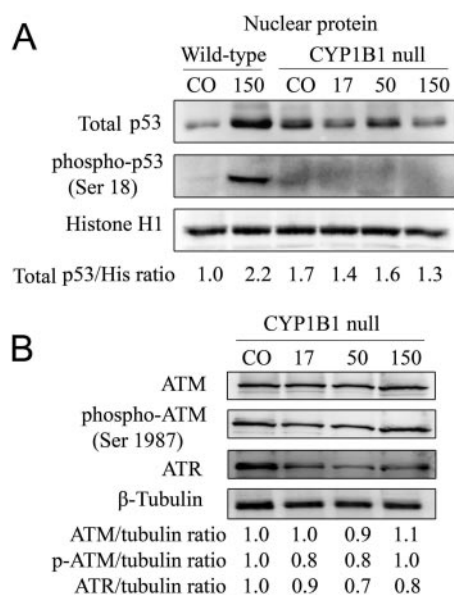


Fig. 3. CYP1B1 deficiency prevents p53 accumulation in nucleus (A). ATM/ATR activity is not altered by DMBA treatments (B). A, p53 protein and phospho-p53 (Ser¹⁸) levels from nucleus portion of CYP1B1-null and WT mice were analyzed by Western blot. Histone H1 was used as protein loading control. The normalized density of lanes is indicated as a ratio at the bottom of the blots. B, ATM, phospho-ATM (Ser¹⁹⁸⁷) and ATR protein levels were analyzed in nuclear protein extractions from CYP1B1-null mice after DMBA and CO treatments. The results were normalized as a ratio to the β -tubulin protein loading control. Representative results are shown in (A and B) for three independent experiments. 17, 50, and 150 indicate 17, 50, and 150 mg/kg DMBA, respectively.

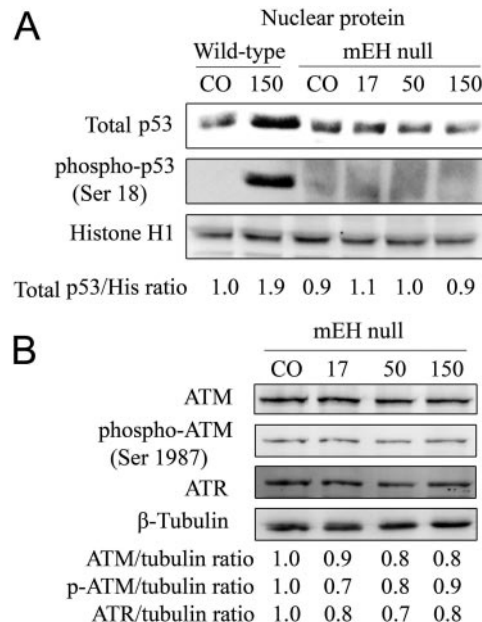


Fig. 4. p53, ATM, and ATR protein levels in spleen cells of mEH-null mice were not altered after DMBA treatments. Nuclear protein extracts from spleens of mEH-null mice and WT mice treated with DMBA were used to determine the level of p53, phospho-p53 (Ser¹⁸) (A), ATM, phospho-ATM (Ser¹⁹⁸⁷), and ATR (B) by Western blot. A, DMBA treatments did not alter the p53 accumulation and activation in the nucleus of spleen cells from mEH-null mice. B, ATM and ATR protein levels were not changed by DMBA treatments in the spleens of mEH-null mice as well. The densitometry results for each band were normalized to histone H1 or β -tubulin. The normalized density of lanes is indicated as a ratio at bottom of the blots. 17, 50, and 150 indicate 17, 50, and 150 mg/kg DMBA, respectively.

and phospho-p53 (Ser¹⁸) cannot be detected in p53-null mice because the upstream translational start site of p53 gene was replaced by neo sequences (Jacks et al., 1994). Total p53 and phospho-p53 (Ser¹⁸) levels were increased in male WT mice by DMBA treatments, and similar responses were observed in female mice (Fig. 2A). To detect the ATM and ATR protein levels in the nucleus of spleen cells from p53-null mice, three individual mouse spleen cell samples from each group were analyzed by Western blot and probed with ATM, phospho-ATM (Ser¹⁹⁸⁷), and ATR antibodies. Each lane on the blot represents one individual mouse sample. After the normalization with loading control and statistical analysis of three samples from each group, we found the levels of ATM and ATR were significantly up-regulated in the 50 mg/kg DMBA dose groups. In addition, the level of phosphorylated ATM (Ser¹⁹⁸⁷) was increased and was shown to be statistically significantly different in the 50 and 150 mg/kg DMBA-treated groups compared with CO. Therefore, because functional p53 is absent in these null mice, we conclude that ATM and ATR act upstream of p53 to sense DMBA-induced DNA damage.

The General Cytotoxic Effects of DMBA in p53-Null Mice and WT Mice. To further investigate the relationship between p53- and DMBA-induced immunosuppression, age-matched male p53-null mice and male WT mice were used for immune function studies. The initial body weights were recorded on the first day of the experiment, and we found no significant body weight difference between groups. After 7 days of dosing, the final body weight and spleen weights were

measured as well. As shown in Table 1, the final body weight in WT and p53-null mice after CO or DMBA treatment produced no significant changes. We observed that the spleen weight was significantly decreased by various DMBA treatments in WT mice (Table 1). Similar effects were observed in our previous studies using female WT mice (Gao et al., 2005). There was no decrease in cell recovery in p53-null mice, indicating that p53 is required for spleen cell cytotoxicity.

We proceeded to investigate the recovered subpopulation of lymphocytes in spleen cells from WT and p53-null mice after CO and various DMBA treatments. Subpopulations of spleen cells were detected by using cell surface marker antibodies. The percentage of cells present in each subset of spleen cells was determined after analysis by flow cytometry. The recovered subpopulations of CD45⁺ spleen cells were calculated and reported as percentage of total cell counts of CD45⁺ cells in each mouse spleen (Fig. 7). DMBA treatments (50 and 150 mg/kg) significantly decreased B cells, pan T cells, T_H cells, cytotoxic T cells, NK cells, and macrophages in WT mice. However, most subpopulations of lymphocytes did not change with DMBA treatment in the p53-null mice. The only observed alteration was the number of B cells detected in mice

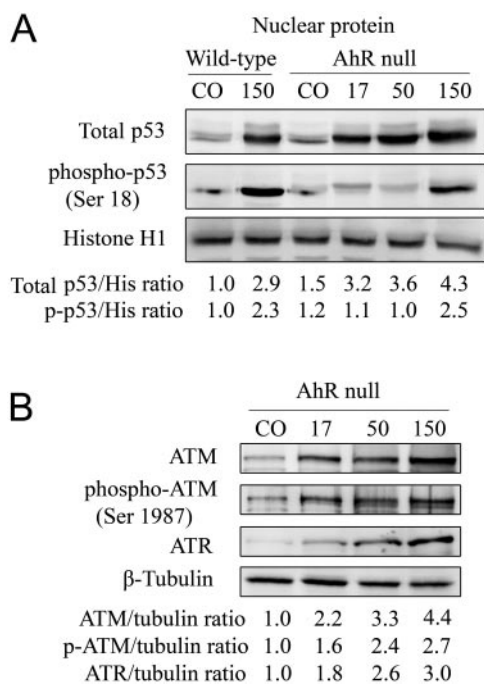


Fig. 5. p53, ATM, ATR protein levels were up-regulated in AhR-null mice after DMBA treatments. A, the p53 and phospho-p53 (Ser¹⁸) protein levels in nuclear fraction were determined by Western blot from AhR-null and WT mice treated with CO or DMBA. Histone H1 was used as a protein loading control. The normalized density of bands is indicated for each treatment as well as for comparative ratios at the bottom of the blots. B, Western blot analysis show that the DMBA treatments increased nuclear ATM, phospho-ATM (Ser¹⁹⁸⁷) and ATR levels in AhR-null mice. β-tubulin was used as a protein loading control. 17, 50, and 150 indicate 17, 50, and 150 mg/kg DMBA, respectively.

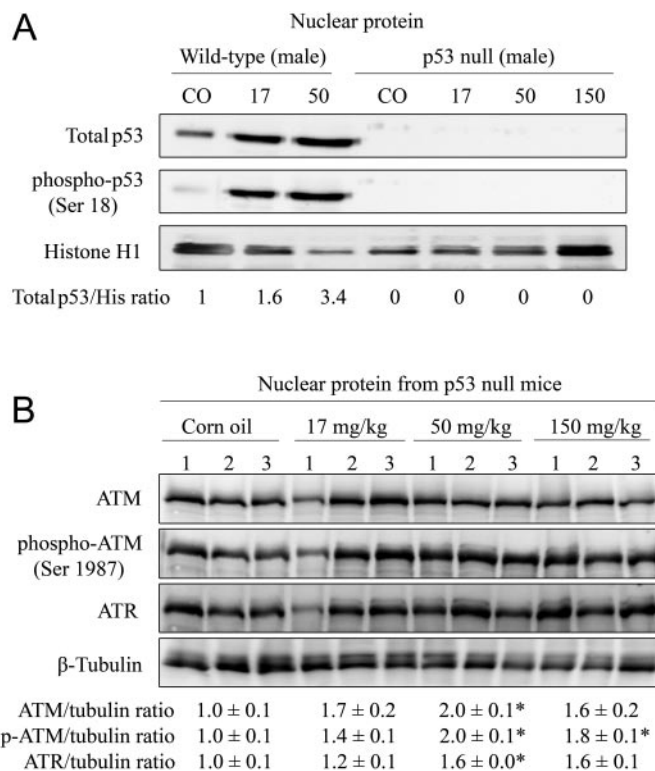


Fig. 6. DMBA altered ATM and ATR activities in male p53-null mice and WT mice. A, male p53-null and male WT mice underwent oral gavage with CO or DMBA as described under *Materials and Methods*. The nuclear p53 and phospho-p53 (Ser¹⁸) were detected by Western blot. No nuclear p53 or phospho-p53 (Ser¹⁸) was observed in p53-null mice after DMBA treatments. Three independent experiments were performed using different individual mouse samples. Similar results were obtained, and representative data are shown. B, the nuclear ATM, phospho-ATM (Ser¹⁹⁸⁷), and ATR protein levels were analyzed by Western blot. Each lane represents an individual mouse sample from each group. Significant increases in ATM and ATR levels were observed in DMBA-treated p53-null mice. The results were normalized to β-tubulin loading control using densitometry and are shown as mean ± S.E.M. of three samples. *, $p < 0.05$, signifies statistically significant difference compared with corn oil control. 17, 50, and 150 indicate 17, 50, and 150 mg/kg DMBA, respectively.

receiving the 150 mg/kg DMBA treatment. Together, these results demonstrate that p53 is required for DMBA to produce general cytotoxic effect in murine spleen cells and that the toxicity of DMBA is not cell lineage-specific.

Effect of DMBA on the Spleen Cell PFC Response in WT and p53-Null Mice. To characterize the DMBA-induced humoral immune response, a T-dependent antibody response and plaque-forming cell assay was performed using in vitro immunization of murine spleen cells with sheep erythrocytes (SRBCs). As we have reported in previous studies, DMBA produced a dose-dependent suppression of the PFC response in WT mice (Fig. 8). In the WT group of mice, the antibody response detected by PFC was nearly eliminated at the 150 mg/kg DMBA dose level, compared with the corn oil control group. In p53-null mice, however, the DMBA treatment with 17 and 50 mg/kg did not change the PFC number compared with the corn oil control. However, a statistically significant suppression occurred in p53-null mice treated with 150 mg/kg DMBA, and the PFC number decreased ~4-fold compared the corresponding corn oil control. Thus, p53 deficiency only partially protects spleen cells from the lower doses of DMBA exposures (17 and 50 mg/kg), suggesting that other non-p53-dependent pathways may also be involved in cytotoxicity. At noncytotoxic doses, these results demonstrate that p53 is required for DMBA-induced immunosuppression.

Effect of DMBA on the Mitogenic Responses of Splenic T and B Cells in WT Mice and p53-Null Mice. [³H]Thymidine incorporation during mitogenesis is an effective method to assess lymphocyte proliferation, which is required for normal immune responses. We have previously shown that DMBA suppresses both T cell proliferation induced by Con A and B cell proliferation induced by LPS in spleen cells (Burchiel et al., 1990). As shown in Fig. 9, DMBA treatments were found to suppress both T and B cell proliferation in a dose-dependent manner in WT mice. A suppressed B cell mitogenic response was observed in p53-null mice after the DMBA treatment as well. For example, the 17 mg/kg dose of DMBA produced a ~50% decrease in the LPS response, whereas there was less than a 10% decrease in the p53-null mice. Likewise, at the 50 mg/kg dose of DMBA, there was greater than 80% suppression in WT mice of the LPS response, whereas p53-null mice were suppressed ~10%. T-cell proliferation was suppressed only by 150 mg/kg DMBA in p53-null mice. These observations demonstrate that the loss of p53 protects T and B cells from immunosuppression at DMBA doses less than 150 mg/kg, as measured by cell proliferation.

DMBA Suppressed NK Cell Activity in WT Mice, but Not in p53-Null Mice. To evaluate the effects of DMBA on

an innate immune response, NK cell activity was assessed using a chromium (⁵¹Cr) release assay (Fig. 10). In the current study, the NK response was suppressed at the 50 and 150 mg/kg levels of DMBA exposure in male WT mice. This finding correlates well with our previously published observations in female WT mice (Gao et al., 2005). DMBA did not alter NK cell activity in p53-null mice except in those mice treated with 150 mg/kg DMBA. A slight increase in NK lysis ability at the 200:1 effector cell/target cell ratio was observed. These results demonstrate that p53 is necessary for DMBA-induced nonspecific immunosuppression as detected using an NK cell assay.

Discussion

In the present studies, we examined the role of genotoxicity produced by DMBA and its dependence on p53, CYP1B1, and mEH enzymes in spleen cell cytotoxicity and immunosuppression. We correlated p53, phospho-p53 (Ser¹⁸), ATM, phospho-ATM (Ser¹⁹⁸⁷), and ATR protein levels in WT, CYP1B1, mEH, AhR, and p53-null mice with immunologic effects. We observed that DMBA can up-regulate these proteins in WT mice, but does not alter them in CYP1B1 or mEH-null mice, suggesting a role for DMBA-DE in ATM/ATR and p53 activation. Our previous data have shown that DMBA-induced immunosuppression is CYP1B1- and mEH-dependent (Gao et al., 2005, 2007). Buters et al. (2003) examined the formation of DMBA-induced DNA adducts in WT and CYP1B1 mice. They found that the total DMBA-DNA-adduct levels in the spleen of female WT mice after 1 week of DMBA treatment (200 μ g/mouse/day, which correlates with our DMBA middle dose) were dramatically higher than those found in other tissues and more than 10-fold higher than the adducts in the spleens of CYP1B1-null mice. Taken together, this observation and our results clearly demonstrate that DMBA needs be metabolically activated by CYP1B1 and mEH to produce genotoxic stress and DNA damage.

It is well known that ATM and ATR are activated by DNA damage (Shiloh, 2003). However, some reports have shown that ATM and ATR might be activated by different types of genotoxic stressors (Yang et al., 2003). ATM responds to double-strand breaks (DSBs), and ATR is primarily activated by UV radiation. In this study, we observed that both ATM and ATR levels were up-regulated after DMBA treatments. Therefore, both kinases can be activated by DMBA-induced genotoxic stress. In our current study, we observed that ATM and ATR were activated in p53-null mice by DMBA, demonstrating that ATM and ATR act upstream of p53 and in concert to phosphorylate p53 at serine 18 in vivo. Recent

TABLE 1

Effect of DMBA on body and spleen weights in WT and p53-null mice

Animals underwent oral gavage with CO or DMBA as described under *Materials and Methods*. The body and spleen weights were recorded at the time of sacrifice on day 7. Values represent mean \pm S.E.M. of five mice per group.

	WT Mice		p53-Null Mice	
	Body Weight	Spleen Weight	Body Weight	Spleen Weight
	g	mg	g	mg
Corn Oil	23.3 \pm 2.1	101.4 \pm 3.3	25.5 \pm 1.0	93.6 \pm 9.4
17 mg/kg DMBA	27.1 \pm 0.9	73.0 \pm 2.3*	24.2 \pm 0.6	104.6 \pm 16.1
50 mg/kg DMBA	27.7 \pm 0.4	54.2 \pm 2.5*	24.0 \pm 0.6	75.6 \pm 3.8
150 mg/kg DMBA	24.7 \pm 0.8	35.0 \pm 1.6*	24.3 \pm 0.7	73.8 \pm 2.8

* $P < 0.05$, signifies statistically significant differences compared to CO control group.

studies have also reported that ATM activation induces the phosphorylation of mdm2 (Khosravi et al., 1999). This ATM-dependent mdm2 phosphorylation can break the p53-mdm2 complex and impair the mdm2 negative effect contributing to stabilization of p53 in vivo (Meek and Knippschild, 2003).

In this report, we observed that phospho-p53 (Ser¹⁸) was significantly increased in murine spleen cells with DMBA treatments. This result is consistent with the report of Chao et al., (2000) who examined various genotoxic chemicals and showed that phosphorylation of murine p53 at serine 18 was in response to DNA damage in mouse embryonic stem cells in vivo. Our studies now show that phosphorylation of this specific site is critical for the p53 response and subsequent DMBA-induced immunosuppression.

DMBA-induced DNA damage can trigger different cell fates such as DNA repair, cell cycle arrest, and apoptosis (Norbury and Hickson, 2001). In a previous study, we observed that most of the recovered subsets of lymphocytes in murine spleens were significantly reduced by apoptotic pathways after DMBA treatments (Burchiel et al., 1992). Page et al. (2003) reported that DMBA treatments induced pre-B cell apoptosis in WT mice but not in p53-null mice. Therefore, we believe that apoptosis is a predominant event for DMBA-induced cytotoxicity in vivo produced at high exposure levels.

Immune function studies from WT and p53-null mice have shown that p53 is a key player in regulating DMBA-induced immunosuppression. However, the suppressive effects observed in the PFC assay and mitogenesis assay in p53-null mice at high doses (150 mg/kg) of DMBA indicate that p53-independent pathways may play important roles in cytotox-

icity and immunosuppression. The p73 protein may play an additional and important role in p53-independent pathways (Melino et al., 2002; Roos and Kaina, 2006). In this pathway, ATM and ATR are activated by DNA damage. E2F1, the downstream transcriptional regulator, is then activated to increase p73 expression. Up-regulated p73 protein can activate the pro-apoptotic gene PUMA or BAX to cause mitochondrial dysfunction and cytochrome *c* release, stimulating the mitochondrial apoptotic pathway (Melino et al., 2004). Immune function studies have shown that DMBA treatments at 17 and 50 mg/kg did not impair the humoral immunity of spleen cells in p53-null mice, indicating that there is a threshold DMBA dose required to trigger the p53-independent pathways in vivo. As shown in Fig. 7, the B cell popu-

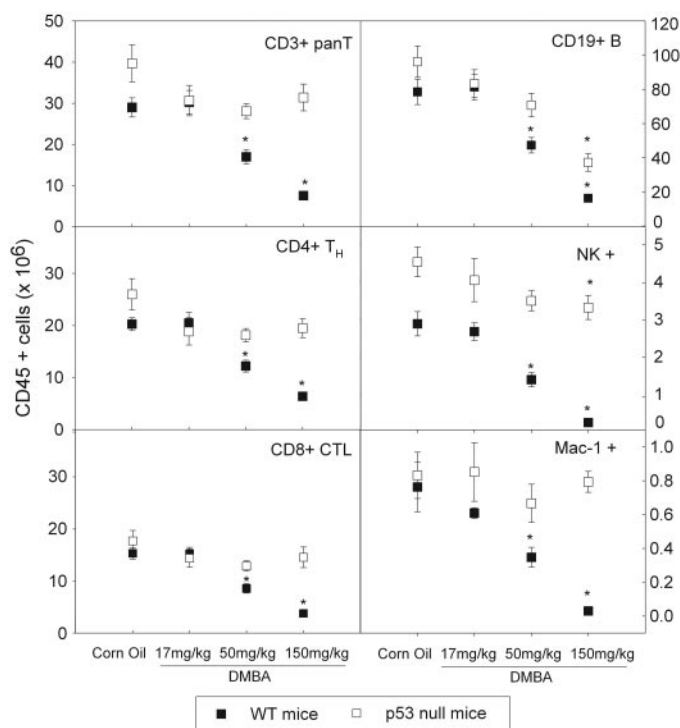


Fig. 7. Recovered subpopulations of CD45⁺ spleen cells in p53-null mice and WT mice after DMBA treatments. As explained in the text, different cell surface markers were used to identify subsets of splenocytes. The error bars are means \pm S.E.M. for five individual mouse samples in each group. *, $p < 0.05$, signifies statistically significant difference compared with the corn oil vehicle control. Data are representative of two experiments.

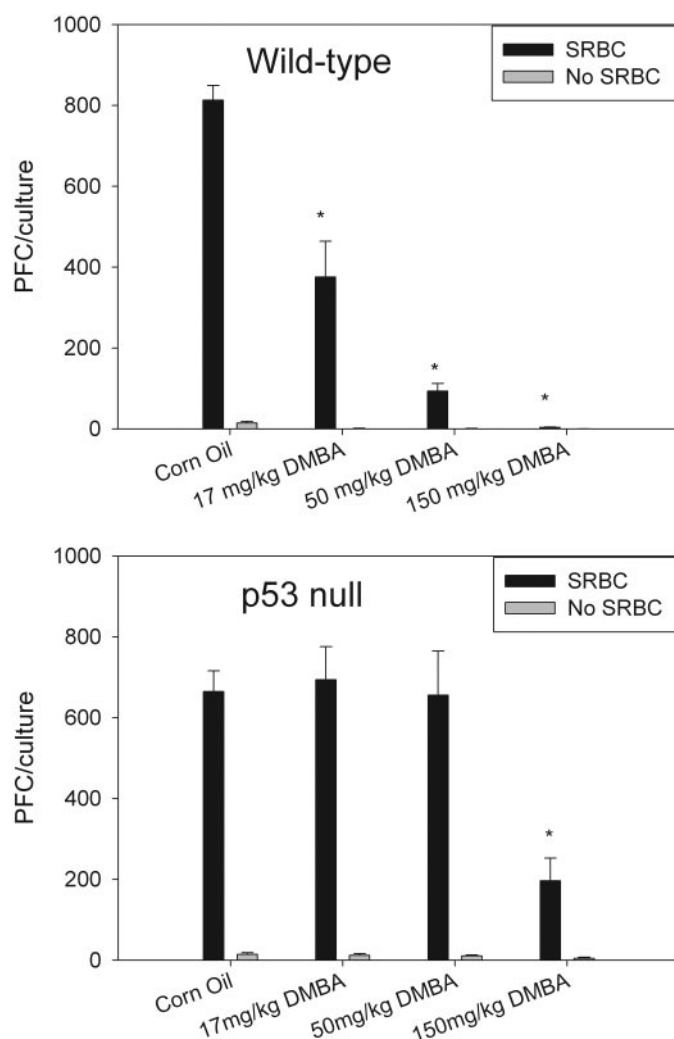


Fig. 8. Effect of DMBA treatment on the primary spleen cell humoral immune (IgM) response to SRBC as determined using a PFC assay in male WT mice and p53-null mice examined ex vivo. Spleen cells were immunized in vitro after removal from mice treated for 5 days with CO or DMBA by oral gavage followed by 48 h of rest. The number of spleen cells producing anti-SRBC response was determined using a modified Jerne and Nordin PFC assay as described under *Materials and Methods*. A, PFC response in WT mice treated with CO or DMBA. B, PFC response in p53-null mice treated with CO or DMBA. Dark bars indicate that cells were immunized with SRBC. Light bars indicate cells plated with complete RPMI media as negative control. Data from five mice in each group assayed individually are shown as mean \pm S.E.M. Statistically significant differences compared with CO are indicated (*, $p < 0.05$). Data are representative of two experiments.

lation was significantly decreased in p53-null mice at the 150 mg/kg DMBA treatment level. Therefore, it is possible that p73 plays an important role in the loss of B cells at high doses of DMBA via p53-independent pathways (Roos and Kaina, 2006).

In this report, AhR-null mice were used to measure the effects of DMBA on p53, ATM, and ATR levels and activation as well. AhR is a very important intracellular receptor that binds with many PAHs to induce gene expression, such as CYP 1A1. However, we have found that DMBA is an extremely weak AhR ligand and that the Ah receptor is probably not important in the spleen cell immunosuppression produced by DMBA (data not shown). Here, we found that p53, phospho-p53 (Ser¹⁸), ATM, phospho-ATM (Ser¹⁹⁸⁷), and ATR levels were increased by DMBA in AhR-null mice. Thus, AhR doses not seem to be important in the p53 response to DMBA of murine spleen cells.

In summary, this study demonstrated that p53 is necessary for DMBA-induced immunosuppression and that ATM

and ATR are activated by DMBA as well. ATM and ATR activation may be implicated in the accumulation of p53 in nucleus and phosphorylation of p53 (Ser¹⁸). In addition, high doses of DMBA may trigger additional p53-independent pathways that are associated with spleen cell cytotoxicity. Therefore, future studies will continue to investigate the role of ATM/ATR and p53 activation in the immunotoxicity of other PAH family members and other chemical agents. Many chemical xenobiotics that induce genotoxicity may activate ATM and ATR, leading to p53 up-regulation as a common mechanism of immunosuppression. The ATM/ATR and p53 activities in the subpopulations of spleen cells need to be characterized for all classes of genotoxic chemicals. Future work focusing on the molecular mechanisms responsible for genotoxic stress-induced immunotoxicity can help us to better understand the potential environmental risk factors associated with the human immune system.

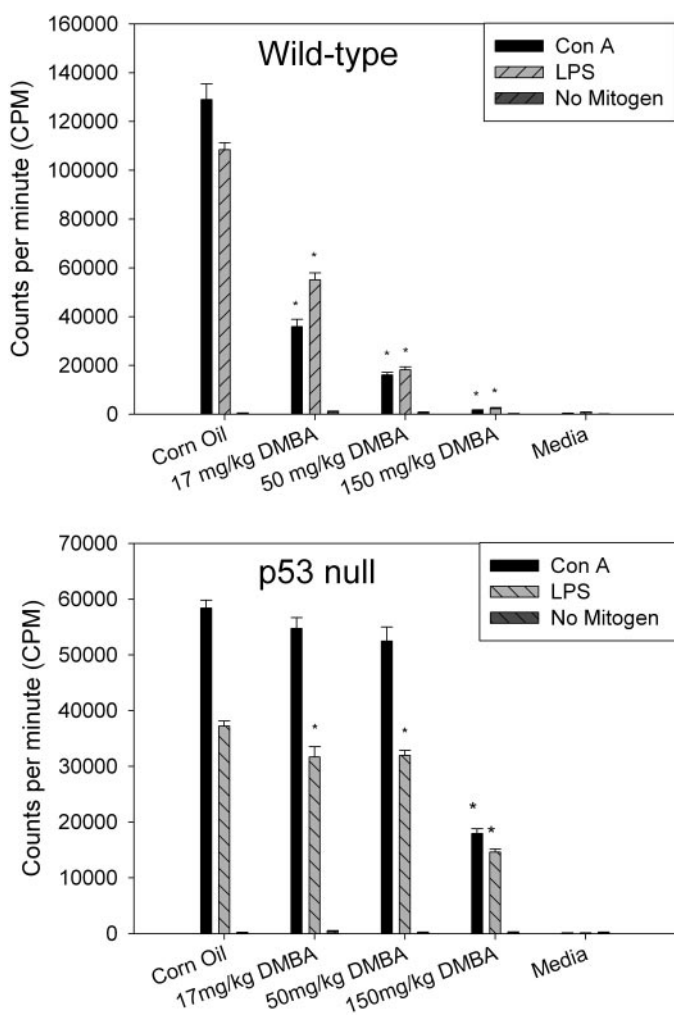


Fig. 9. Effect of DMBA on the mitogenic response of splenic T and B cells in male WT mice and p53-null mice examined ex vivo. Spleen cells were cultured with LPS (B cells), Con A (T cells), or no mitogen (complete RPMI 1640 medium) as control. The mitogenic response was assessed on the basis of [³H] incorporation into DNA. Values are means \pm S.E.M. of 5 individual mouse samples per group; each sample was assayed in replicates of six. *, $p < 0.05$, signifies statistically significant difference compared with corn oil control. Data are representative of two experiments.

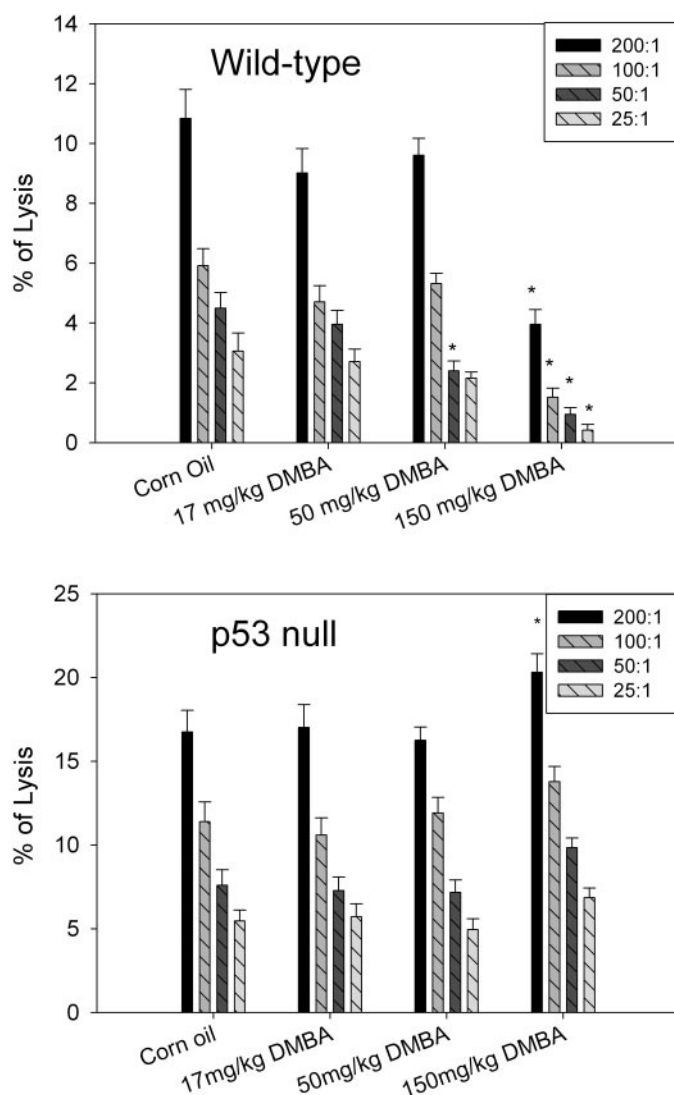


Fig. 10. Effect of DMBA on NK cell activity in male WT mice and male p53-null mice. The NK assay was performed at different effector (E) cell (NK cells) to ⁵¹Cr labeled target (T) cell (Yac-1) ratios indicated in the box insets. Data are means \pm S.E.M. of triplicate cultures from five individual mice samples in each group. *, $p < 0.05$, signifies statistically significant difference compared with the CO control group. Independent experiments were performed twice.

Acknowledgments

We thank Drs. Craig Marcus, Ke Jian Liu, and Chien-An Hu for their scientific advice and direction in these studies.

References

- Appella E and Anderson CW (2001) Post-translational modifications and activation of p53 by genotoxic stresses. *Eur J Biochem* **268**:2764–2772.
- Bakkenist CJ and Kastan MB (2003) DNA damage activates ATM through intermolecular autophosphorylation and dimer dissociation. *Nature* **421**:499–506.
- Banin S, Moyal L, Shieh S, Taya Y, Anderson CW, Chessa L, Smorodinsky NI, Prives C, Reiss Y, Shiloh Y, et al. (1998) Enhanced phosphorylation of p53 by ATM in response to DNA damage. *Science* **281**:1674–1677.
- Burchiel SW, Davis DA, Gomez MP, Montano RM, Barton SL, and Seamer LC (1990) Inhibition of lymphocyte activation in splenic and gut-associated lymphoid tissues following oral exposure of mice to 7,12-dimethylbenz[a]anthracene. *Toxicol Appl Pharmacol* **105**:434–442.
- Burchiel SW, Davis DA, Ray SD, Archuleta MM, Thilsted JP, Corcoran GB (1992) DMBA-induced cytotoxicity in lymphoid and nonlymphoid organs of B6C3F1 mice: relation of cell death to target cell intracellular calcium and DNA damage. *Toxicol Appl Pharmacol* **113**:126–132.
- Buters J, Quintanilla-Martinez L, Schober W, Soballa VJ, Hintermair J, Wolff T, Gonzalez FJ, and Greim H (2003) CYP1B1 determines susceptibility to low doses of 7,12-dimethylbenz[a]anthracene-induced ovarian cancers in mice: correlation of CYP1B1-mediated DNA adducts with carcinogenicity. *Carcinogenesis* **24**:327–334.
- Buters JT, Sakai S, Richter T, Pineau T, Alexander DL, Savas U, Doehmer J, Ward JM, Jefcoate CR, and Gonzalez FJ (1999) Cytochrome P450 CYP1B1 determines susceptibility to 7,12-dimethylbenz[a]anthracene-induced lymphomas. *Proc Natl Acad Sci U S A* **96**:1977–1982.
- Canman CE, Lim DS, Cimprich KA, Taya Y, Tamai K, Sakaguchi K, Appella E, Kastan MB, and Siliciano JD (1998) Activation of the ATM kinase by ionizing radiation and phosphorylation of p53. *Science* **281**:1677–1679.
- Caspari T (2000) How to activate p53. *Curr Biol* **10**:R315–317.
- Chao C, Saito S, Anderson CW, Appella E, and Xu Y (2000) Phosphorylation of murine p53 at ser-18 regulates the p53 responses to DNA damage. *Proc Natl Acad Sci U S A* **97**:11936–11941.
- Dertinger SD, Nazarenko DA, Silverstone AE, and Gasiewicz TA (2001) Aryl hydrocarbon receptor signaling plays a significant role in mediating benzo[a]pyrene- and cigarette smoke condensate-induced cytogenetic damage in vivo. *Carcinogenesis* **22**:171–177.
- Dipple A and Nebzydowski JA (1978) Evidence for the involvement of a diol-epoxide in the binding of 7,12-dimethylbenz[a]anthracene to DNA in cells in culture. *Chem Biol Interact* **20**:17–26.
- Gao J, Lauer FT, Dunaway S and Burchiel SW (2005) Cytochrome P450 1B1 is required for 7,12-dimethylbenz[a]anthracene (DMBA) induced spleen cell immunotoxicity. *Toxicol Sci* **86**:68–74.
- Gao J, Lauer FT, Mitchell LA, and Burchiel SW (2007) Microsomal epoxide hydrolase is required for 7,12-dimethylbenz[a]anthracene (DMBA) induced immunotoxicity in mice. *Toxicol Sci* **98**:137–144.
- Gately DP, Hittle JC, Chan GK, and Yen TJ (1998) Characterization of ATM expression, localization, and associated DNA-dependent protein kinase activity. *Mol Biol Cell* **9**:2361–2374.
- Heidel SM, MacWilliams PS, Baird WM, Dashwood WM, Buters JT, Gonzalez FJ, Larsen MC, Czuprynski CJ, and Jefcoate CR (2000) Cytochrome P4501B1 mediates induction of bone marrow cytotoxicity and preleukemia cells in mice treated with 7,12-dimethylbenz[a]anthracene. *Cancer Res* **60**:3454–3460.
- Hickman ES, Moroni MC, and Helin K (2002) The role of p53 and pRB in apoptosis and cancer. *Curr Opin Genet Dev* **12**:60–66.
- Ikegwonu FI, Christou M, and Jefcoate CR (1999) Regulation of cytochrome P4501B1 (CYP1B1) in mouse embryo fibroblast (C3H10T1/2) cells by protein kinase C (PKC). *Biochem Pharmacol* **57**:619–630.
- Jacks T, Remington L, Williams BO, Schmitt EM, Halachmi S, Bronson RT, and Weinberg RA (1994) Tumor spectrum analysis in p53-mutant mice. *Curr Biol* **4**:1–7.
- Keegan KS, Holtzman DA, Plug AW, Christenson ER, Brainerd EE, Flaggs G, Bentley NJ, Taylor EM, Meyn MS, Moss SB, et al. (1996) The Atr and Atm protein kinases associate with different sites along meiotically pairing chromosomes. *Genes Dev* **10**:2423–2437.
- Khosravi R, Maya R, Gottlieb T, Oren M, Shiloh Y, and Shkedy D (1999) Rapid ATM-dependent phosphorylation of MDM2 precedes p53 accumulation in response to DNA damage. *Proc Natl Acad Sci U S A* **96**:14973–14977.
- Kurz EU and Lees-Miller SP (2004) DNA damage-induced activation of ATM and ATM-dependent signaling pathways. *DNA Repair (Amst)* **3**:889–900.
- Lakin ND and Jackson SP (1999) Regulation of p53 in response to DNA damage. *Oncogene* **18**:7644–7655.
- Lavin MF, Birrell G, Chen P, Kozlov S, Scott S, and Gueven N (2005) ATM signaling and genomic stability in response to DNA damage. *Mutation Res* **569**:123–132.
- Meek DW and Knippschild U (2003) Posttranslational modification of MDM2. *Mol Cancer Res* **1**:1017–1026.
- Melino G, Bernassola F, Ranalli M, Yee K, Zong WX, Corazzari M, Knight RA, Green DR, Thompson C, and Vousden KH (2004) p73 Induces apoptosis via PUMA transactivation and Bax mitochondrial translocation. *J Biol Chem* **279**:8076–8083.
- Melino G, De Laurenzi V, and Vousden KH (2002) p73: friend or foe in tumorigenesis. *Nat Rev Cancer* **2**:605–615.
- Miyata M, Kudo G, Lee YH, Yang TJ, Gelboin HV, Fernandez-Salguero P, Kimura S, and Gonzalez FJ (1999) Targeted disruption of the microsomal epoxide hydrolase gene. Microsomal epoxide hydrolase is required for the carcinogenic activity of 7,12-dimethylbenz[a]anthracene. *J Biol Chem* **274**:23963–23968.
- Myers JS and Cortez D (2006) Rapid activation of ATR by ionizing radiation requires ATM and Mre11. *J Biol Chem* **281**:9346–9350.
- Norbury CJ and Hickson ID (2001) Cellular responses to DNA damage. *Annu Rev Pharmacol Toxicol* **41**:367–401.
- Page TJ, O'Brien S, Holston K, MacWilliams PS, Jefcoate CR, and Czuprynski CJ (2003) 7,12-Dimethylbenz[a]anthracene-induced bone marrow toxicity is p53-dependent. *Toxicol Sci* **74**:85–92.
- Pelkonen O and Nebert DW (1982) Metabolism of polycyclic aromatic hydrocarbons: etiologic role in carcinogenesis. *Pharmacol Rev* **34**:189–222.
- Prives C and Hall PA (1999) The p53 pathway. *J Pathol* **187**:112–126.
- Roos WP and Kaina B (2006) DNA damage-induced cell death by apoptosis. *Trends Mol Med* **12**:440–450.
- Shiloh Y (2003) ATM and related protein kinases: safeguarding genome integrity. *Nat Rev Cancer* **3**:155–168.
- Sugiyama T, Osaka M, Koami K, Maeda S, and Ueda N (2002) 7,12-DMBA-induced rat leukemia: a review with insights into future research. *Leuk Res* **26**:1053–1068.
- Thurmond LM, House RV, Lauer LD, and Dean JH (1988) Suppression of splenic lymphocyte function by 7,12-dimethylbenz[a]anthracene (DMBA) in vitro. *Toxicol Appl Pharmacol* **93**:369–377.
- Tibbetts RS, Brumbaugh KM, Williams JM, Sarkaria JN, Cliby WA, Shieh SY, Taya Y, Prives C, and Abraham RT (1999) A role for ATR in the DNA damage-induced phosphorylation of p53. *Genes Dev* **13**:152–157.
- Uno S, Dalton TP, Derkenne S, Curran CP, Miller ML, Shertzer HG, and Nebert DW (2004) Oral exposure to benzo[a]pyrene in the mouse: detoxication by inducible cytochrome P450 is more important than metabolic activation. *Mol Pharmacol* **65**:1225–1237.
- Yang J, Yu Y, Hamrick HE, and Duerksen-Hughes PJ (2003) ATM, ATR and DNA-PK: initiators of the cellular genotoxic stress responses. *Carcinogenesis* **24**:1571–1580.

Address correspondence to: Dr. Scott W. Burchiel, College of Pharmacy, 1 University of New Mexico, MSC09 5360, Albuquerque, NM 87131. E-mail: sburchiel@salud.unm.edu